Physics Letters B 686 (2010) 199–206

Contents lists available at ScienceDirect

Physics Letters B

www.elsevier.com/locate/physletb

Holographic conductivity of zero temperature superconductors

R.A. Konoplya [a,b], A. Zhidenko [c,*]

[a] Department of Physics, Kyoto University, Kyoto 606-8501, Japan
[b] Theoretical Astrophysics, Eberhard-Karls University of Tübingen, Ti
[c] Instituto de Física, Universidade de São Paulo, C.P. 66318, 05315-970, São Paulo-SP, Brazil

ARTICLE INFO

Article history:
Received 11 November 2009
Received in revised form 16 January 2010
Accepted 12 February 2010
Available online 20 February 2010
Editor: M. Cvetič

ABSTRACT

Using the recently found by G. Horowitz and M. Roberts (arXiv:0908.3677) numerical model of the ground state of holographic superconductors (at zero temperature), we calculate the conductivity for such models. The universal relation connecting conductivity with the reflection coefficient was used for finding the conductivity by the WKB approach. The dependence of the conductivity on the frequency and charge density is discussed. Numerical calculations confirm the general arguments of (arXiv:0908.3677) in favor of non-zero conductivity even at zero temperature. In addition to the Horowitz–Roberts solution we have found (probably infinite) set of extra solutions which are normalizable and reach the same correct RN-AdS asymptotic at spatial infinity. These extra solutions (which correspond to larger values of the grand canonical potential) lead to effective potentials that also vanish at the horizon and thus correspond to a non-zero conductivity at zero temperature.

1. Introduction

The famous AdS/CFT correspondence [1] allows to describe conformal field theory in d-dimensional space–time by considering a $(d+1)$-dimensional super-gravity in anti-de Sitter space–time. This opens a number of opportunities to look into non-perturbative quantum field theory at strong coupling. One of the recent interesting applications of such a holography is constructing of a model of a superconductor. Usually in quantum field theory superconductors are well understood by the Bardeen–Cooper–Schrieffer, theory [2], though there are indications that for some systems the standard Fermi liquid theory cannot be a good approximation [3]. Therefore a holographic model for superconductors was suggested by Hartnoll, Herzog and Horowitz [4]. This model have been recently studied in a number of papers and some alternative models of holographic superconductors were suggested [5–36]. These models contain a charged asymptotically anti-de Sitter black hole which have non-trivial hairs at low temperatures. Until recent time, there were suggested various holographic models for the low temperature limit, while the dual description for the actual zero temperature ground state remained unknown. The very recent paper of Horowitz and Roberts [38] solves this problem and find numerically the zero temperature holographic dual for superconductors.

The system under consideration consists of the charged scalar field coupled to a charged $(3+1)$-dimensional black hole, so that above some critical temperature, in the normal phase, the system is described by the Reissner–Nordström–anti-de Sitter black holes, while below the critical temperature, in the super-conducting phase, the black hole develops scalar hairs. Thus, the superconductor is $(2+1)$-dimensional, what might be realized for instance in graphene. In [38], based on qualitative arguments, it has been shown that the effective potential of the perturbation equation for the dynamic of the Maxwell field vanishes at the horizon, and, consequently, the conductivity never vanishes even at zero temperature. Though some intuitive arguments were given in [38] about the behavior of conductivity in the suggested model, no calculations of conductivity were performed there, except for some estimations made for the low-frequency regime. Therefore our first aim here was to calculate conductivity for the Horowitz–Roberts model [38]. When integrating the field equations, in addition to the ground state solution described in [38], we have found a number of other solutions with the same leading AdS asymptotic at spatial infinity and obeying the same general form of ansatz near the horizon. We have checked that the found here extra solutions, as that of [38], have vanishing effective potential at the horizon, so that the conductivity will never be zero even at zero temperature. They correspond to configurations of the scalar field with higher energies at zero temperature.

The Letter is organized as follows. Section 2 gives the basics equations for the system of fields under consideration and scheme of construction of the numerical solution for a black hole with the scalar hair. Section 3 describes the spectrum of the obtained solu-

* Corresponding author.
E-mail addresses: konoplya_roma@yahoo.com (R.A. Konoplya), zhidenko@fma.if.usp.br (A. Zhidenko).

0370-2693 © 2010 Elsevier B.V. Open access under CC BY license.
doi:10.1016/j.physletb.2010.02.048

tions which consists of the ground state solution and solutions of the higher grand canonical potential. Section 4 is devoted to WKB calculations of the conductivity for the zero-temperature superconductor.

2. Construction of the Horowitz–Roberts holographic dual

The Lagrangian density for the system under consideration takes the form

$$\mathcal{L} = R + \frac{6}{L^2} - \frac{1}{4}F^{\mu\nu}F_{\mu\nu} - |\nabla\psi - iqA\psi|^2 - U\big(|\psi|\big) \tag{1}$$

where ψ is the scalar field, $F_{\mu\nu}$ is the strength tensor of electromagnetic field, m, q are the scalar field's charge and mass and A is the vector-potential ($F = dA$). The cosmological constant is $-3/L^2$. The plane symmetric solution can written in a general form

$$ds^2 = -g(r)e^{-\chi(r)}dt^2 + \frac{dr^2}{g(r)} + r^2\big(dx^2 + dy^2\big), \tag{2}$$

$$A = \phi(r)\,dt, \qquad \psi = \psi(r). \tag{3}$$

We shall fix the gauge so that ψ is real and measure all the quantities in units of the AdS radius, so that $L = 1$. The equations have the form:

$$\psi'' + \left(\frac{g'}{g} - \frac{\chi'}{2} + \frac{2}{r}\right)\psi' + \frac{q^2\phi^2 e^{\chi}}{g^2}\psi - \frac{U'(\psi)}{2g} = 0, \tag{4a}$$

$$\phi'' + \left(\frac{\chi'}{2} + \frac{2}{r}\right)\phi' - \frac{2q^2\psi^2}{g}\phi = 0, \tag{4b}$$

$$\chi' + r\psi'^2 + \frac{rq^2\phi^2\psi^2 e^{\chi}}{g^2} = 0, \tag{4c}$$

$$g' + \left(\frac{1}{r} - \frac{\chi'}{2}\right)g + \frac{r\phi'^2 e^{\chi}}{4} - 3r + \frac{rU(\psi)}{2} = 0. \tag{4d}$$

When we choose $\chi = 0$ at infinity, the metric takes the standard AdS form at larger r.

$$\phi = \mu - \frac{\rho}{r}, \qquad \psi = \frac{\psi^{(\lambda)}}{r^{\lambda}} + \frac{\psi^{(3-\lambda)}}{r^{3-\lambda}}, \tag{5}$$

where $\lambda = (3 + \sqrt{9 + 4m^2})/2$. In the boundary dual CFT, μ is the chemical potential, ρ is the charge density, and λ is the scaling dimension of the operator dual to ψ. We used

$$\psi^{(3-\lambda)} = 0. \tag{6}$$

The density of the grand canonical potential Ω of the state that corresponds to a given solution can be find by fitting the function $g(r)$ at large r [37]

$$e^{-\chi(r)}g(r) = r^2 + \frac{\Omega}{r} + o\left(\frac{1}{r}\right). \tag{7}$$

Let us consider two cases:

1. The case $m^2 = 0$ corresponds to a marginal operator, $\lambda = 3$, in the $2+1$ superconductor with a non-zero expectation value. Following [38] we have used the ansatz

$$\phi = r^{2+\alpha}, \qquad \psi = \psi_0 - \psi_1 r^{2(1+\alpha)},$$
$$\chi = \chi_0 - \chi_1 r^{2(1+\alpha)}, \qquad g = r^2\big(1 - g_1 r^{2(1+\alpha)}\big). \tag{8}$$

The coefficients in ϕ and g can be taken equal to unity. Substituting this into the field equations and equating the dominant terms for small r (with $\alpha > -1$), one has

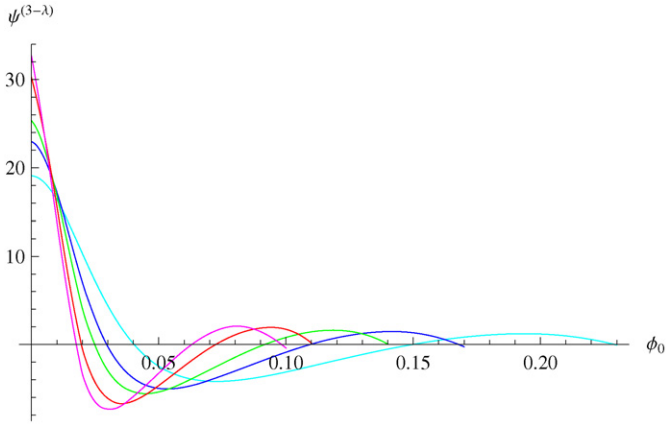

Fig. 1. Dependence of the coefficient $\psi^{(3-\lambda)}$ on ϕ_0 for $m^2 = -2$ ($\lambda = 2$) $q = 2$ for various staring points of integration $\epsilon = 1/500$ (cyan), $\epsilon = 1/2000$ (blue), $\epsilon = 1/5000$ (green), $\epsilon = 1/20000$ (red), $\epsilon = 1/50000$ (magenta). The smaller value of ϵ is the closer zeros of $\psi^{(3-\lambda)}$ are located. (For interpretation of the references to colour in this figure legend, the reader is referred to the web version of this Letter.)

$$q\psi_0 = \left(\frac{\alpha^2 + 5\alpha + 6}{2}\right)^{1/2},$$
$$\chi_1 = \frac{\alpha^2 + 5\alpha + 6}{4(\alpha + 1)}e^{\chi_0}, \qquad g_1 = \frac{\alpha + 2}{4}e^{\chi_0},$$
$$\psi_1 = \frac{qe^{\chi_0}}{2\big(2\alpha^2 + 7\alpha + 5\big)}\left(\frac{\alpha^2 + 5\alpha + 6}{2}\right)^{1/2}. \tag{9}$$

These formulas were obtained in [38].
We solve Eqs. (4) numerically using the ansatz (8). We choose α in order to satisfy the condition (6) using the shooting algorithm.

2. In [38] the ansatz for small r has been found for the case of $m^2 < 0$ and $q^2 > -m^2/6$ ($\lambda < 3$):

$$\phi = \phi_0 r^{\beta}\big(-\ln(r)\big)^{1/2}, \qquad \psi = 2\big(-\ln(r)\big)^{1/2},$$
$$\chi = \chi_0 + \ln\big(-\ln(r)\big), \qquad g = \big(2m^2/3\big)r^2\ln(r), \tag{10}$$

where

$$\beta = -\frac{1}{2} + \sqrt{1 - \frac{48q^2}{m^2}} > 1.$$

Unfortunately, we were unable to construct a convergent procedure of integration in this case. We used the following method. We started the integration of (4) from some point ϵ which is very close to the horizon $r = 0$, substituting as an initial condition the ansatz (10). Then we decreased the value of ϵ and compare the results. We did not observe the convergence of the functions when decreasing ϵ. Namely, as ϵ approached zero the functions did not approach a certain limit, showing significantly different behavior. In Fig. 1 we can see the dependence of the coefficient $\psi^{(3-\lambda)}$ on the parameter ϕ_0 for various values of ϵ. We checked that neither zeros of $\psi^{(3-\lambda)}$ converge as $\epsilon \to 0$ and, therefore, we were not able to find the appropriate value of ϕ_0 for the solution that satisfies (6). We have checked also that addition of sub-dominant terms to the ansatz (10) does not remedy the situation.

The $m = 0$ case is free from the above problem of absence of convergence and from here and on we shall consider only this case.

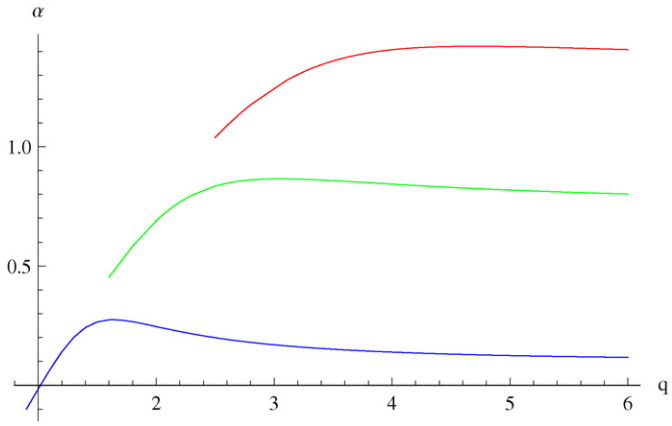

Fig. 2. Three lowest solutions for $m=0$ given by α as functions of q.

Eqs. (4) have the two-parametric symmetry [38]

$$r \to ar, \qquad t \to \frac{b}{a}t, \qquad g \to a^2 g,$$
$$\phi \to \frac{a}{b}\phi, \qquad e^{\chi} \to b^2 e^{\chi}. \tag{11}$$

One of these parameters allows us to fix $\chi(r\to\infty)=0$. The other parameter re-scales the parameters of the solutions and can be chosen so that the chemical potential is unit.

In order to satisfy these two conditions, after the solution is found we choose

$$b = e^{-\chi(\infty)/2}, \qquad a = b/\mu.$$

After this re-scaling the solution does not depend on the value of χ_0 and we can take $\chi_0 = 0$.

3. Spectrum of the solutions

In [38], a value of α satisfying (6) was found for $m=0$ as a function of q. It is interesting to note, that for each fixed q this value of α is not unique. At least for large values of q, there is a discrete spectrum of values of α. Each of these value of α (under the same fixed q) corresponds to a *different solution* of (4) that satisfies the condition (6). The dependence $q(\alpha)$ for the first three solutions is shown in Fig. 2. We have checked that for all of the above three curves the solutions are normalizable and reach their AdS asymptotic at large distance. Near $r=0$, all three solutions obey the same general ansatz (8) though certainly with different values of α for each q. Although we have demonstrated only three solutions of the spectrum, it looks as if there is an infinite spectrum of solutions with increasing values of α for a fixed q.

In Fig. 4 we see how the coefficient $\psi^{(3-\lambda)}$ depends on α and on q: when α grows, the zeros of $\psi^{(3-\lambda)}$ become more and more dense in α, and when q grows the he zeros of $\psi^{(3-\lambda)}$ become more spaced. Therefore different solutions (i.e. different lines $q(\alpha)$) lay closer to each other for smaller q and larger α making it difficult to distinguish numerically different nearby solutions. That is why the two upper curves do not continue in Fig. 2 to the region where they probably coincide or lay very close to each other: the numerical integration is not easy in that region as there are probably many other solutions nearby. We believe however that accurate numerical integration could allow to complete at least a few upper curves until the minimal value of q.

For larger α we observe that another singular point appears for $r>0$ (see Fig. 5).

The above found solutions correspond to *lower* energy states of the superconductor (see Fig. 3). In order to see this, we find the density of the grand canonical potential for the corresponding states by fitting (7). Then, we can calculate the density of the free energy, using the formula

$$F = \Omega + \mu\rho. \tag{12}$$

We found that Ω is larger for the state with larger α, but the free energy F appears to be lower (see caption for Fig. 6).

In order to check our numerical calculations of the thermodynamical potentials, we use the following relation between the grand canonical potential and the free energy

$$2\Omega = -F. \tag{13}$$

This relation can be easily derived from (5.11) of [37] in the limit of zero temperature and magnetic field. We find that (13) is satisfied up to the numerical precision.

In Fig. 2 one can see the three smallest values of α for which (6) is satisfied. The smallest α is the one found by Horowitz and Roberts. All the potentials are positive definite, vanish at the horizon ($z=-\infty$) and at the spatial infinity ($z=0$). The potential for the lowest value of α has one peak. The effective potential for the nth higher value of α has n peaks (Fig. 6). The larger value of α corresponds to the state with larger charge density ρ larger absolute value of the scalar hair $\psi^{(\lambda)}$ and lower density of the free energy.

4. Conductivity by the WKB method

Assuming translational symmetry and stationary ansatz in time, the linearized perturbation of the vector potential satisfies the wave-like equation [37]

$$A_x'' + \left(\frac{g'}{g} - \frac{\chi'}{2}\right)A_x' + \left(\left(\frac{\omega^2}{g^2} - \frac{\phi'^2}{g}\right)e^{\chi} - \frac{2q^2\psi^2}{g}\right)A_x = 0. \tag{14}$$

Using a new radial variable $dz = \frac{e^{\chi/2}}{g}dr$, at large r, $dz = dr/r^2$, and we choose the constant of integration so that $z=-1/r$. The horizon is located at $z=-\infty$. Then (14) has the wave-like form:

$$-A_{x,zz} + V(z)A_x = \omega^2 A_x, \tag{15}$$

where the effective potential [38]

$$V(z) = g\left[\phi_{,r}^2 + 2q^2\psi^2 e^{-\chi}\right]. \tag{16}$$

As was shown in [38] this effective potential always vanishes at the horizon. Since we consider only solutions which satisfy (6), the potential also vanishes at the spatial infinity.

In terms of non-rescaled functions the potential and the tortoise coordinate are given by

$$V(r) = \frac{a^2}{b^2}g\left(\phi_{,r}^2 + 2q^2\psi^2 e^{-\chi}\right) = \frac{g}{\mu^2}\left(\phi_{,r}^2 + 2q^2\psi^2 e^{-\chi}\right),$$
$$dz = \frac{b}{a}\frac{e^{\chi/2}}{g}dr = \frac{e^{\chi/2}}{\mu g}dr. \tag{17}$$

According to the Horowitz–Roberts interpretation, the holographic conductivity can be expressed in terms of the reflection coefficients [38] in the following way. In order to solve (15) with the ingoing wave boundary conditions at $z=-\infty$ we can extend the definition of the effective potential to positive z by setting $V=0$ for $z>0$ (the boundary of the anti-de Sitter space (spatial infinity) is located at $z=0$).

Now an incoming wave from the right will be partly transmitted and partly reflected by the potential barrier. The transmitted

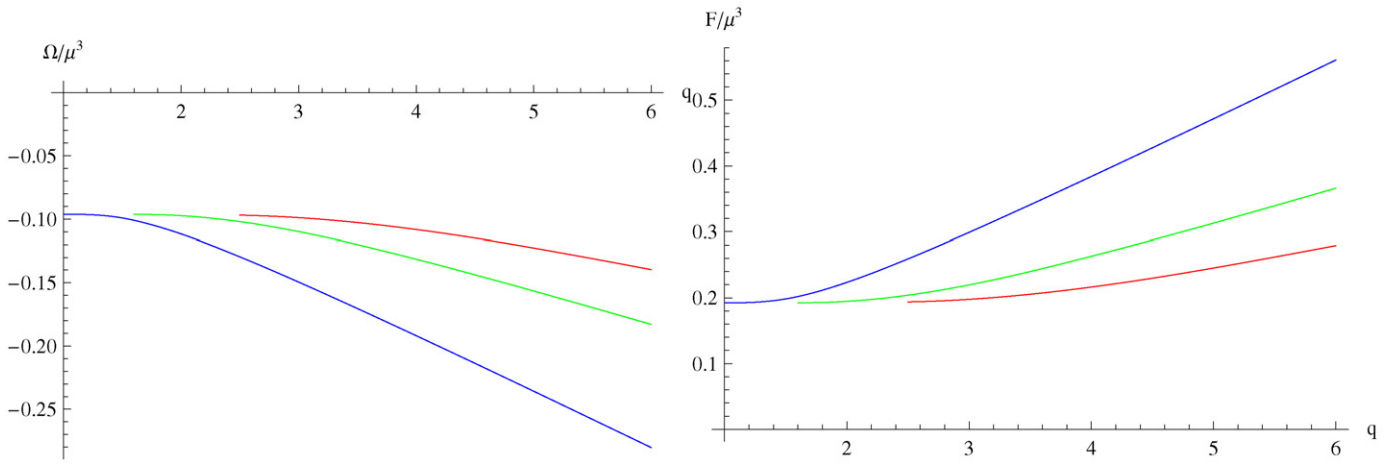

Fig. 3. The densities of the grand canonical potential (left figure) and the free energy (right figure) for the three lowest solutions for $m = 0$ as functions of q.

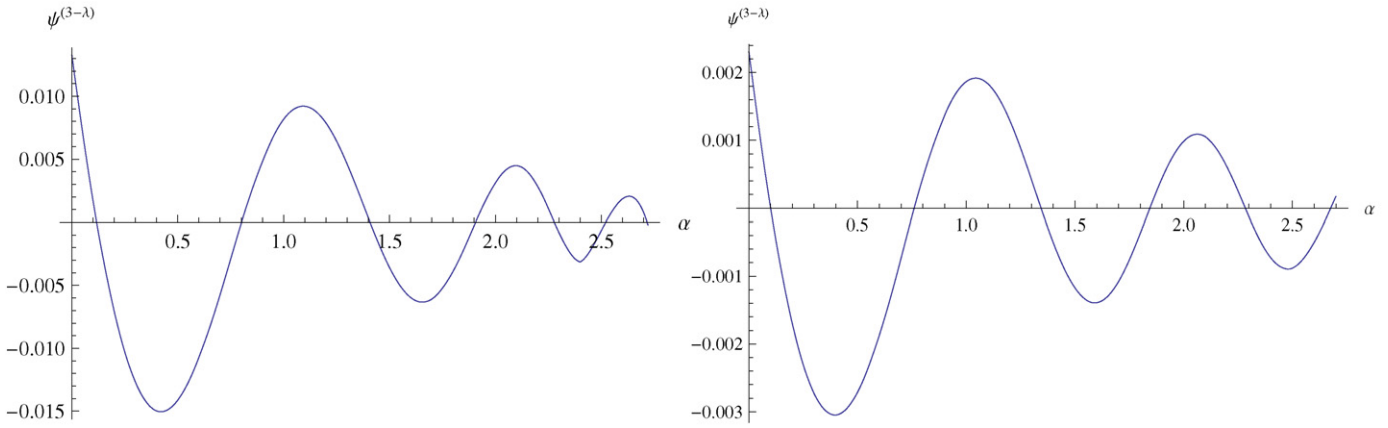

Fig. 4. Dependence of the coefficient $\psi^{(3-\lambda)}$ on α for $q = 6$ (left) and $q = 30$ (right).

wave is purely ingoing at the horizon and the reflected wave satisfies the scattering boundary conditions at $z \to \infty$. Thus the scattering boundary conditions for $z > 0$ are

$$A_x = e^{-i\omega z} + Re^{i\omega z}, \quad z \to +\infty, \tag{18}$$

and at the event horizon

$$A_x = Te^{-i\omega z}, \quad z \to -\infty, \tag{19}$$

where R and T are reflection and transmission coefficients. Then one has

$$A_x(0) = 1 + R, \qquad A_{x,z}(0) = -i\omega(1 - R). \tag{20}$$

As shown in [4], if $A_x = A_x^{(0)} + A_x^{(1)}/r$, and the conductivity is

$$\sigma(\omega) = -\frac{i}{\omega}\frac{A_x^{(1)}}{A_x^{(0)}}. \tag{21}$$

Since $A_x^{(1)} = -A_{x,z}(0)$, so

$$\sigma(\omega) = \frac{1 - R}{1 + R}. \tag{22}$$

The above boundary conditions (18), (19) are nothing but the standard scattering boundary conditions for finding the S-matrix. The effective potential has the distinctive form of the potential barrier, so that the WKB approach [39] can be applied for finding R and σ. Let us note, that as the wave energy (or frequency) ω is real, the first order WKB values for R and T will be real [39] and

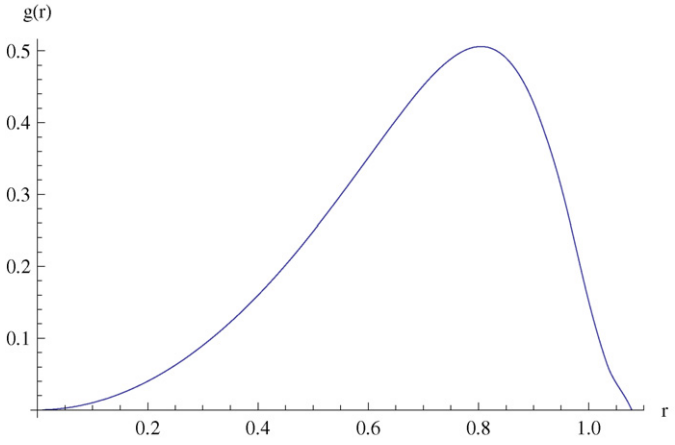

Fig. 5. Another singular point in the metric function $g(r)$ at $r > 0$ when α in the ansatz (8) is large ($m = 0$, $q = 6$, $\alpha = 2.8$).

$$T^2 + R^2 = 1. \tag{23}$$

Next, we shall distinguish the two qualitatively different cases: first, when ω^2 is much less then the maximum of the effective potential $\omega^2 \ll V_0$, and second when ω^2 is of the same order that the maximum of the potential $\omega^2 \simeq V_0$ and can be either greater

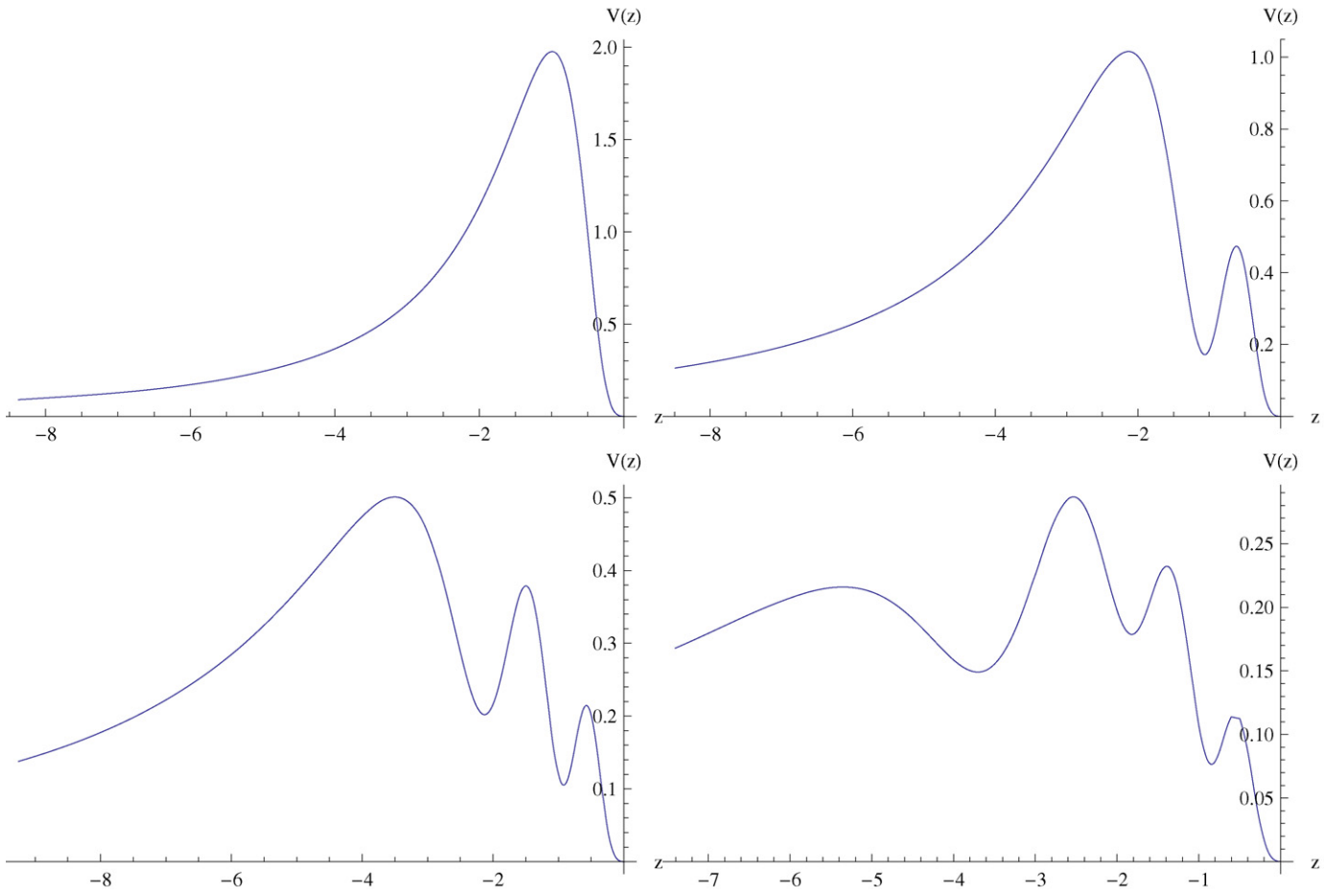

Fig. 6. The effective potentials as functions of the corresponding tortoise coordinates for $m = 0$, $q = 6$ ($\lambda = 3$) that for the four smallest values of α:

α	ρ/μ^2	$\psi^{(\lambda)}/\mu^\lambda$	Ω/μ^3	F/μ^3
0.117	0.84	0.79	−0.28	0.56
0.802	0.55	−0.58	−0.18	0.37
1.408	0.42	0.42	−0.14	0.28
1.907	0.35	−0.31	−0.12	0.24

or smaller than the maximum. Strictly speaking, we should have to consider also the third case when ω^2 is much larger than the maximum of the potential, but, as we shall see in most cases the reflection coefficient R decreases too quickly with ω, so that σ reaches its maximal value (unity) even at moderate $\omega > V_0$.

For $\omega^2 \approx V_0$, we shall use the first order beyond the eikonal approximation WKB formula, developed by B. Schutz and C. Will (see [39]) for scattering around black holes

$$R = \left(1 + e^{-2i\pi(\nu+(1/2))}\right)^{-\frac{1}{2}}, \quad \omega^2 \simeq V_0, \tag{24}$$

where

$$\nu + \frac{1}{2} = i\frac{(\omega^2 - V_0)}{\sqrt{-2V_0''}} + \Lambda_2 + \Lambda_3. \tag{25}$$

Here V_0'' is the second derivative of the effective potential in its maximum, Λ_2 and Λ_3 are second and third WKB corrections which depend on up to sixth order derivatives of the effective potential at its maximum,

$$\Lambda_2 = \frac{1}{(2Q_0'')^{1/2}}\left\{\frac{1}{8}\left(\frac{Q_0^{(4)}}{Q_0''}\right)\left(\frac{1}{4} + N^2\right) - \frac{1}{288}\left(\frac{Q_0'''}{Q_0''}\right)^2\left(7 + 60N^2\right)\right\}, \tag{26}$$

$$\begin{aligned}\Lambda_3 = \frac{N}{(2Q_0'')^{1/2}}\Bigg\{&\frac{5}{6912}\left(\frac{Q_0'''}{Q_0''}\right)^4\left(77 + 188N^2\right) \\ &- \frac{1}{384}\left(\frac{Q_0'''^2 Q_0^{(4)}}{Q_0''^3}\right)\left(51 + 100N^2\right) \\ &+ \frac{1}{2304}\left(\frac{Q_0^{(4)}}{Q_0''}\right)^2\left(67 + 68N^2\right) \\ &+ \frac{1}{288}\left(\frac{Q_0''' Q_0^{(5)}}{Q_0''^2}\right)\left(19 + 28N^2\right) \\ &- \frac{1}{288}\left(\frac{Q_0^{(6)}}{Q_0''}\right)\left(5 + 4N^2\right)\Bigg\},\end{aligned} \tag{27}$$

and

$$N = \nu + \frac{1}{2}, \qquad Q_0^{(n)} = \left.\frac{d^n Q}{dr_*^n}\right|_{r_* = r_*(r_{max})},$$

$$Q \equiv \omega^2 - V.$$

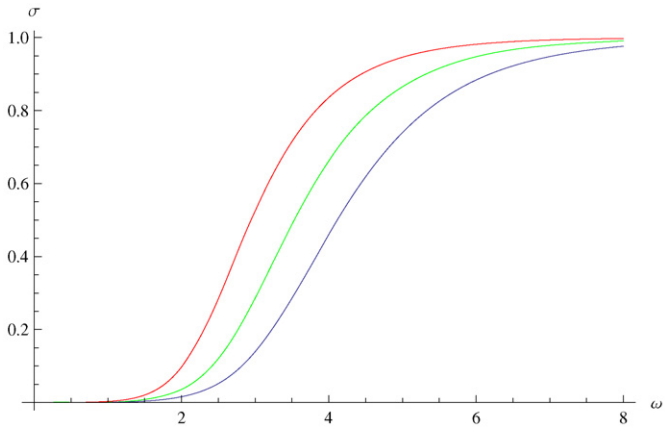

Fig. 7. The conductivity found by the WKB formula for $q = 10$ (top, red), $q = 12$ (green), $q = 14$ (bottom, blue) as a function of frequency ω for $m = 0$.

The above formula was extended up to the sixth WKB order in [40] and applied to a number of problems of scattering around black holes (see for instance [41] and references therein). Mainly it was used for finding the so-called quasinormal modes of black holes, which imply special boundary conditions, so that ν becomes integer in that case. For arbitrary ν and each given ω the above WKB formula works for problems with the standard scattering boundary conditions. We shall look for higher WKB orders in order to have the idea of possible order of the error in the obtained results. Though the WKB series converges only asymptotically, in many cases, quite unexpectedly, WKB values have region of relative convergence in orders.

The case of small frequencies is well described by the well-known formula

$$T = e^{-\int_{z_1}^{z_2} dz \sqrt{V(z)-\omega^2}}, \quad \omega^2 \ll V_0 \tag{28}$$

i.e. the at small frequency the transmission is exponentially suppressed. Here z_1 and z_2 are the turning points for which $V(z) = \omega^2$. The reflection coefficient follows from (23)

$$R = \sqrt{1 - e^{-2\int_{z_1}^{z_2} dz \sqrt{V(z)-\omega^2}}}, \quad \omega^2 \ll V_0. \tag{29}$$

At small frequencies the reflection coefficient is close to 1, i.e. almost all energy is reflected by the potential. Then R decreases with the increasing of ω, and, for sufficiently large ω, usually seemingly larger than V_0 or about it, the reflection coefficient is close to zero. This means that according to (22), the conductivity changes from zero at small frequencies until 1 at large frequencies. This kind of behavior we can see in Fig. 7, where the conductivity was obtained by using and the expression (22) and the WKB formula (29) (for $\omega \leqslant 0.4$) and (24) (for $\omega \geqslant 0.4$). There one can see that as ω^2 approaches the peak of the potential barrier (which is located at $r \approx 0.18$), the accuracy of the formula (29) diminishes and (24) becomes a better approximation. Though a good confirmation of consistency of the both approximations (29) and (24) is the possibility of "smooth matching" of both data (see Figs. 8, 9) if neglecting small intermediate region of ω, where both approximation have marginal accuracy (for Fig. 2, this intermediate region is $0.3 \leqslant \omega \leqslant 0.4$). In some range of parameters, such as the one shown in Fig. 3 (right), there is no such intermediate region that should be neglected but, even better, both regimes (29) and (24) overlap, giving almost the same values for some range of large values of q.

Let us note here two important technical points. First is that when using formula (29) one needs the higher order derivatives of the effective potential which is unknown in analytical form, but is given only numerically. It would be a rough method to approximate the effective potential by some interpolating analytical function and then to take derivatives of it: each derivative would bring additional numerical error to the calculations. Instead we used the field equations (4) and have taken all necessary derivatives from (4) and by taking the corresponding derivatives of the wave and metric functions ϕ, ψ, g, etc.

Another important moment is the accuracy of the used WKB technique. The existence of the "common region" where both formulas produce the same result says that for large values of q the WKB formulas work very well (Fig. 10). The analysis of the higher order corrections indeed shows that for large q (and $\omega^2 \simeq V_0$) the WKB series shows convergence in a few first orders: An example is $q = 10$, $\omega = 2.2$, $R = 0.778$ for the first WKB order, $R = 0.722$ for second WKB order, and $R = 0.725$ for the third order. This gives estimated error of less than one percent. There is no such good convergence for small values of q, therefore for $\omega^2 \simeq V_0$ we have used here the WKB formula of the first order for small q, and third order formula for large q.

At small frequencies we have obtained a close, though not coinciding, numerical result to the formula (3.21) of [38]

$$\sigma = \left(\frac{\omega}{\omega_0}\right)^{\delta}, \qquad \delta = \sqrt{4V_0 + 1} - 1. \tag{30}$$

Thus for $q = 1.6$, we obtained by WKB $\delta \approx 4.8$ ($\omega_0 = 0.45$), what is close to $\sqrt{4V_0+1} - 1 \approx 4.55$, while for $q = 1$ WKB gives $\delta \approx 3.0$ ($\omega_0 \approx 1.3$) and $\sqrt{4V_0+1} - 1 \approx 3.97$. The WKB correction to the (30), as it can be seen from the above data, may be quite big and about 25 per cents.

The formula (30) used for its derivation rough matching of the left and right dominant asymptotics. Thus it is expected to be less accurate than the WKB method we are using here.

5. Conclusions

We have found the WKB values of conductivity for the Horowitz–Roberts model of the zero-temperature superconductor for $m^2 = 0$ case. Dependence of conductivity on parameters of the theory such as the charge density ρ and the frequency ω is investigated. WKB data for conductivity confirms the qualitative arguments that σ does not reach zero even at zero temperature, in agreement with [38]. By the WKB calculations we have confirmed the analytic relation derived in [38] for the ω-dependence of σ at small frequencies and calculated the pre-factor for this relation for various q. The used here third order WKB formula which has very good accuracy for large values of q (and moderate ω), showing convergence in orders with an estimated error of around fractions of one percent. In addition, we have found the set of other solutions which describe the superconductor at zero temperature in the states with higher grand canonical potential and lower energy.

Our Letter may be improved in a number of ways. First of all, the conductivity values could be obtained with better accuracy, if one uses the numerical shooting, which is known to work well for asymptotically AdS space–times [42]. The conductivity of higher grand potential states with $m = 0$ cannot be obtained by WKB formula we used, because the effective potentials for higher states have a number of local maximums. Thus accurate shooting approach would allow also for complete analysis of conductivities of these states. Finally, the case of non-vanishing mass of the scalar field m probably requires some other and more sophisticated procedure of integration or a different ansatz near the horizon from that suggested in [38].

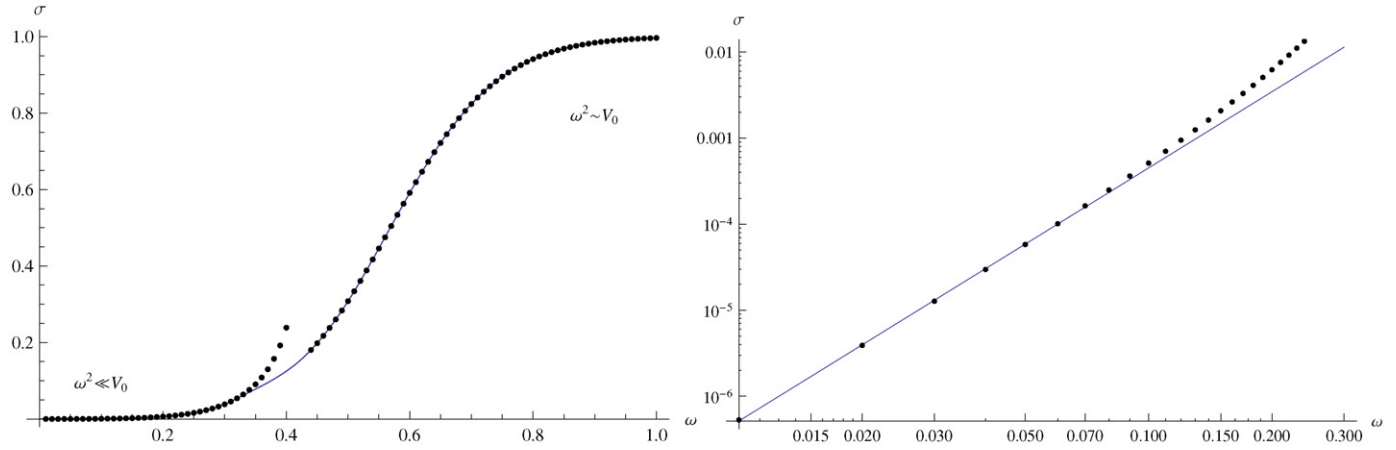

Fig. 8. The conductivity for $m = 0$, $q = 1$ as a function of frequency ω ($\delta \approx 3.0$). In the left figure the solid line corresponds to the interpolation between the two WKB approximations (24) and (29). In the right figure the solid line corresponds to the fit of the numerical data for small values of ω.

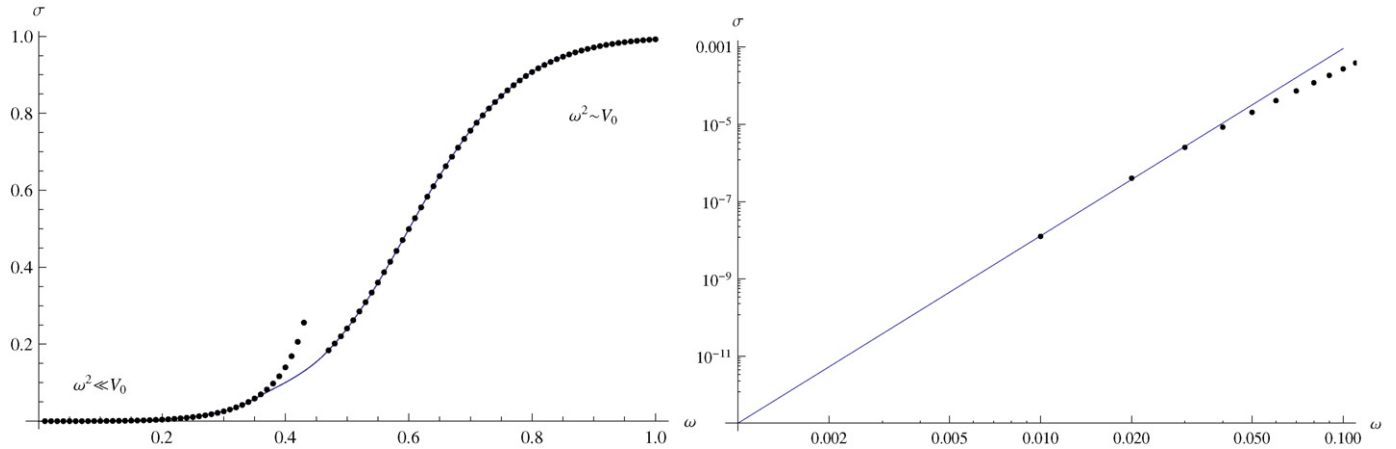

Fig. 9. The conductivity for $m = 0$, $q = 1.6$ as a function of frequency ω ($\delta \approx 4.8$). In the left figure the solid line corresponds to the interpolation between the two WKB approximations (24) and (29). In the right figure the solid line corresponds to the fit of the numerical data for small values of ω.

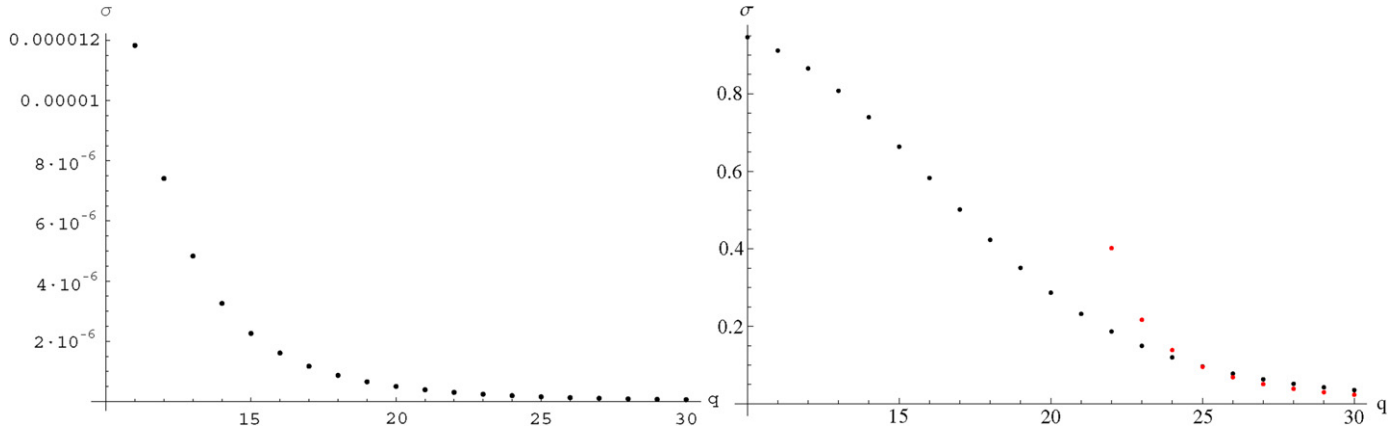

Fig. 10. WKB conductivity for $m = 0$ and for various values q, $\omega = 1/2$ (left) and $\omega = 5$ (right). As q grows, the maximum of the effective potential grows, so that a fixed ω moves down from the peak, approaching the regime $\omega^2 \ll V_0$ (red dots). (For interpretation of the references to colour in this figure legend, the reader is referred to the web version of this Letter.)

Acknowledgements

At the initial stage of this work R.A.K. was supported by *the Japan Society for the Promotion of Science* (JSPS), Japan and at the final stage by *the Alexander von Humboldt foundation* (AvH), Germany. A.Z. was supported by *Fundação de Amparo à Pesquisa do Estado de São Paulo (FAPESP)*, Brazil. A.Z. also acknowledges the hospitality of the University of Guadalajara, México, where a part of this work was done.

References

[1] J.M. Maldacena, Adv. Theor. Math. Phys. 2 (1998) 231, Int. J. Theor. Phys. 38 (1999) 1113, arXiv:hep-th/9711200.
[2] J. Bardeen, L.N. Cooper, J.R. Schrieffer, Phys. Rev. 108 (1957) 1175.
[3] E.W. Carlson, V.J. Emery, S.A. Kivelson, D. Orgad, Concepts in high temperature superconductivity, arXiv:cond-mat/0206217.
[4] S.A. Hartnoll, C.P. Herzog, G.T. Horowitz, Phys. Rev. Lett. 101 (2008) 031601, arXiv:0803.3295 [hep-th].
[5] E.J. Brynjolfsson, U.H. Danielsson, L. Thorlacius, T. Zingg, arXiv:0908.2611 [hep-th].
[6] S.S. Gubser, A. Nellore, arXiv:0908.1972 [hep-th].
[7] S.S. Gubser, S.S. Pufu, F.D. Rocha, arXiv:0908.0011 [hep-th].
[8] J.P. Gauntlett, J. Sonner, T. Wiseman, arXiv:0907.3796 [hep-th].
[9] S.S. Gubser, C.P. Herzog, S.S. Pufu, T. Tesileanu, arXiv:0907.3510 [hep-th].
[10] R. Gregory, S. Kanno, J. Soda, arXiv:0907.3203 [hep-th].
[11] O.C. Umeh, JHEP 0908 (2009) 062, arXiv:0907.3136 [hep-th].
[12] K. Peeters, J. Powell, M. Zamaklar, arXiv:0907.1508 [hep-th].
[13] M. Montull, A. Pomarol, P.J. Silva, arXiv:0906.2396 [hep-th].
[14] H.b. Zeng, Z.y. Fan, Z.z. Ren, arXiv:0906.2323 [hep-th].
[15] T. Albash, C.V. Johnson, arXiv:0906.1795 [hep-th].
[16] S. Franco, A. Garcia-Garcia, D. Rodriguez-Gomez, arXiv:0906.1214 [hep-th].
[17] T. Albash, C.V. Johnson, arXiv:0906.0519 [hep-th].
[18] Y. Kim, Y. Ko, S.J. Sin, arXiv:0904.4567 [hep-th].
[19] C.P. Herzog, J. Phys. A 42 (2009) 343001, arXiv:0904.1975 [hep-th].
[20] K. Maeda, M. Natsuume, T. Okamura, Phys. Rev. D 79 (2009) 126004, arXiv:0904.1914 [hep-th].
[21] S. Pu, S.J. Sin, Y. Zhou, arXiv:0903.4185 [hep-th].
[22] D.f. Zeng, arXiv:0903.2620 [hep-th].
[23] I. Amado, M. Kaminski, K. Landsteiner, JHEP 0905 (2009) 021, arXiv:0903.2209 [hep-th].
[24] J. Sonner, arXiv:0903.0627 [hep-th].
[25] G. Koutsoumbas, E. Papantonopoulos, G. Siopsis, JHEP 0907 (2009) 026, arXiv:0902.0733 [hep-th].
[26] A. O'Bannon, JHEP 0901 (2009) 074, arXiv:0811.0198 [hep-th].
[27] P. Basu, J. He, A. Mukherjee, H.H. Shieh, arXiv:0810.3970 [hep-th].
[28] M. Ammon, J. Erdmenger, M. Kaminski, P. Kerner, arXiv:0810.2316 [hep-th].
[29] M.M. Roberts, S.A. Hartnoll, JHEP 0808 (2008) 035, arXiv:0805.3898 [hep-th].
[30] S.S. Gubser, S.S. Pufu, JHEP 0811 (2008) 033, arXiv:0805.2960 [hep-th].
[31] T. Albash, C.V. Johnson, JHEP 0809 (2008) 121, arXiv:0804.3466 [hep-th].
[32] E. Nakano, W.Y. Wen, Phys. Rev. D 78 (2008) 046004, arXiv:0804.3180 [hep-th].
[33] S.A. Hartnoll, arXiv:0903.3246 [hep-th].
[34] G.T. Horowitz, M.M. Roberts, Phys. Rev. D 78 (2008) 126008, arXiv:0810.1077 [hep-th].
[35] K. Maeda, T. Okamura, Phys. Rev. D 78 (2008) 106006, arXiv:0809.3079 [hep-th].
[36] D. Minic, J.J. Heremans, arXiv:0804.2880 [hep-th].
[37] S.A. Hartnoll, C.P. Herzog, G.T. Horowitz, JHEP 0812 (2008) 015, arXiv:0810.1563 [hep-th].
[38] G.T. Horowitz, M.M. Roberts, arXiv:0908.3677 [hep-th].
[39] B.F. Schutz, C.M. Will, Astrophys. J. Lett. 291 (1985) L33.
[40] S. Iyer, C.M. Will, Phys. Rev. D. 35 (1987) 3621;
R.A. Konoplya, J. Phys. Stud. 8 (2004) 93;
R.A. Konoplya, Phys. Rev. D 68 (2003) 024018, arXiv:gr-qc/0303052.
[41] J. Grain, A. Barrau, Nucl. Phys. B 742 (2006) 253, arXiv:hep-th/0603042;
P. Kanti, R.A. Konoplya, Phys. Rev. D 73 (2006) 044002, arXiv:hep-th/0512257;
H. Kodama, R.A. Konoplya, A. Zhidenko, arXiv:0904.2154 [gr-qc];
S.K. Chakrabarti, Eur. Phys. J. C 61 (2009) 477, arXiv:0809.1004 [gr-qc];
Y. Zhang, Y.X. Gui, F. Yu, Chin. Phys. Lett. 26 (2009) 030401, arXiv:0710.5064 [gr-qc].
[42] R.A. Konoplya, A. Zhidenko, Phys. Rev. D 78 (2008) 104017, arXiv:0809.2048 [hep-th].